






A novel transposable element-based authentication protocol for *Drosophila* cell lines

Daniel Mariyappa ^{1,†}, Douglas B. Rusch,^{2,†} Shunhua Han ³, Arthur Luhur ¹, Danielle Overton,^{1,‡} David F. B. Miller,² Casey M. Bergman ^{3,4} and Andrew C. Zelfhof ^{1,*}

¹Biology Department, Drosophila Genomics Resource Center, Indiana University, Bloomington, IN 47405, USA,

²Biology Department, Center for Genetics and Bioinformatics, Indiana University, Bloomington, IN 47405, USA,

³Department of Genetics and Institute of Bioinformatics, University of Georgia, Athens, GA 30602, USA, and

⁴Department of Genetics, University of Georgia, Athens, GA 30602, USA

*Corresponding author: Email: azelhof@indiana.edu

†These authors contributed equally to this work.

‡Present address: Biology Department, Indiana University–Purdue University Indianapolis, Indianapolis, IN 46202, USA.

Abstract

Drosophila cell lines are used by researchers to investigate various cell biological phenomena. It is crucial to exercise good cell culture practice. Poor handling can lead to both inter- and intra-species cross-contamination. Prolonged culturing can lead to introduction of large- and small-scale genomic changes. These factors, therefore, make it imperative that methods to authenticate *Drosophila* cell lines are developed to ensure reproducibility. Mammalian cell line authentication is reliant on short tandem repeat (STR) profiling; however, the relatively low STR mutation rate in *Drosophila melanogaster* at the individual level is likely to preclude the value of this technique. In contrast, transposable elements (TEs) are highly polymorphic among individual flies and abundant in *Drosophila* cell lines. Therefore, we investigated the utility of TE insertions as markers to discriminate *Drosophila* cell lines derived from the same or different donor genotypes, divergent sub-lines of the same cell line, and from other insect cell lines. We developed a PCR-based next-generation sequencing protocol to cluster cell lines based on the genome-wide distribution of a limited number of diagnostic TE families. We determined the distribution of five TE families in S2R+, S2-DRSC, S2-DGRC, Kc167, ML-DmBG3-c2, mbn2, CME W1 Cl.8+, and ovarian somatic sheath *Drosophila* cell lines. Two independent downstream analyses of the next-generation sequencing data yielded similar clustering of these cell lines. Double-blind testing of the protocol reliably identified various *Drosophila* cell lines. In addition, our data indicate minimal changes with respect to the genome-wide distribution of these five TE families when cells are passaged for at least 50 times. The protocol developed can accurately identify and distinguish the numerous *Drosophila* cell lines available to the research community, thereby aiding reproducible *Drosophila* cell culture research.

Keywords: transposable element; *Drosophila*; cell lines; authentication

Introduction

As of 2018, the estimated number of publications using all cell culture studies is ~2 million (Bairoch 2018). However, problems with reproducibility and authenticity hamper their use (Almeida et al. 2016). Poor culture practices in individual laboratories have led to many cases of inter- and intra-species cross-contamination (Capes-Davis et al. 2010). Additionally, prolonged passaging can lead to large- and small-scale genomic changes due to *in vitro* evolution that cause sub-lines of the same cell line to vary among laboratories (Ben-David et al. 2018; Liu et al. 2019). For example, extensive passaging (>50 passages) of viral-transformed human lymphoblastoid cell lines is associated with increased genotypic instability (Oh et al. 2013). Likewise, long-term passaging of mammalian cell lines is known to lead to increased single nucleotide variations (Pavlova et al. 2015), reduced differentiation potential (Yang et al. 2018), and changes in the karyotype (Wenger et al. 2004). To overcome these inconsistencies

in experiments across laboratories when using human cell lines, the American National Standards Institute and the American Type Culture Collection (ANSI/ATCC ASN-002) have provided a standard for vertebrate cell culture work. Moreover, the NIH offers guidelines for authenticating key research resources that have been endorsed by several major journals (ATCC 2011; NIH 2015; NIH Rigor and Reproducibility 2014).

Though most of the above-mentioned problems and solutions relate to mammalian cell culture practice, a significant number of laboratories use *Drosophila* cells for basic research. *Drosophila* cell lines are used by researchers to investigate a myriad of cellular processes including receptor–ligand interactions (Ozkan et al. 2013), cellular signaling (Albert and Bokel 2017), circadian biology (Albert and Bokel 2017), metal homeostasis (Mohr et al. 2018), cellular stress response (Aguilera-Gomez et al. 2017), neurobiology (Tsuyama et al. 2017), innate immunity (Nonaka et al. 2017), and functional genomics (Albert and Bokel 2017), as well as being

Received: August 13, 2021. Accepted: November 11, 2021

© The Author(s) 2021. Published by Oxford University Press on behalf of Genetics Society of America.

This is an Open Access article distributed under the terms of the Creative Commons Attribution License (<https://creativecommons.org/licenses/by/4.0/>), which permits unrestricted reuse, distribution, and reproduction in any medium, provided the original work is properly cited.

used extensively for gene editing by CRISPR Cas9 technology (Luhur *et al.* 2019). Furthermore, as part of the modENCODE project, the transcriptional and chromatin profiles of a large panel of *Drosophila* cell lines were determined to facilitate studies on gene function and expression (Cherbas *et al.* 2011; Kharchenko *et al.* 2011). However, currently there are no protocols available to authenticate *Drosophila* cell lines. In addition, the effects of long-term passaging on *Drosophila* cell lines have not been formally investigated despite evidence for extensive changes from wild-type ploidy and copy number in many *Drosophila* cell lines (Zhang *et al.* 2010; Lee *et al.* 2014), implying that insect cells can potentially exhibit genomic changes in culture like their mammalian counterparts.

Human cell line authentication guidelines recommend short tandem repeat (STR) profiling as the method of choice for routine cell typing, although approaches using genomic techniques yield more comprehensive information (Almeida *et al.* 2016). The use of STR profiling as the preferred method to authenticate human cell lines is based on high STR allelic diversity among the donors for different cell lines, relatively low cost, stability of using STR markers, and the historical availability of methods to assay STR variants during the development of human cell line authentication protocols. There are a number of limitations with the STR approach. The ANSI/ATCC ASN-002 standard for typing human cell lines with STRs is over 100 pages long and requires careful implementation for proper interpretation. Moreover, STR-based methods for human cell line authentication are primarily designed to discriminate cell lines derived from different donors, but are less powerful for discriminating cell lines or sub-lines from the same donor genotype.

Development of cell line authentication protocols requires understanding the genome biology of a species, the specific characteristics of the most widely used cell lines in that research community, and how these features can be used to leverage cost-effective modern genomic technologies. In *Drosophila*, the majority of widely-used cell lines have been derived from a limited number of donor genotypes. Coupled with the low STR mutation rate in *Drosophila* relative to humans (Schug *et al.* 1997), the use of STR profiling for discriminating different *Drosophila* cell lines is likely to be limited. In contrast, it is well-established that transposable elements (TEs) are highly polymorphic among individual flies or between inbred strains (Charlesworth and Langley 1989; Cridland *et al.* 2013) and that *Drosophila* cell lines have an increased TE abundance relative to whole flies (Potter *et al.* 1979; Rahman *et al.* 2015). These properties, together with the large number of potential insertion sites across the genome and stability of TE insertions at individual loci, suggest that TE insertions should theoretically be useful markers to simultaneously discriminate *Drosophila* cell lines made from different donor genotypes as well as from the same donor genotype, including divergent sub-lines of the same cell line. Han *et al.* (2021) recently tested this prediction and demonstrated that genome-wide TE insertion profiles can reliably cluster different *Drosophila* cell lines from the same donor genotypes and discriminate cell lines from different donor genotypes, while also preserving information about the laboratory of origin. A minimal subset of six active TE families (297, *copia*, *mdg3*, *mdg1*, *roo*, and 1731) was also determined to have essentially the same discriminative power as the genome-wide dataset (Han *et al.* 2021). These six TE families are all long terminal repeat (LTR) retrotransposons, which are the most abundant type of TE in *Drosophila* cell lines (Rahman *et al.* 2015) and are typically composed of recently active insertions

with highly similar sequences (Bergman and Bensasson 2007), features which potentially enhance their use as markers.

Based upon these findings, we investigated if the genome-wide distribution of these six TE families could form the basis for a reliable protocol to authenticate *Drosophila* cell lines. As noted earlier, several of the modENCODE cell lines are extensively used to study genomic and cell biological processes (Cherbas *et al.* 2011; Kharchenko *et al.* 2011). These cell lines are also amongst the most widely-ordered cell lines from *Drosophila* Genomics Resource Center (DGRC). Therefore, we used six modENCODE lines derived from various *Drosophila melanogaster* developmental stages: S2R+, S2-DRSC, Kc167 (embryonic origin); ML-DmBG3-c2 (L3 larval CNS origin); *mbn2* (larval circulatory system origin); and CME W1 Cl.8+ (wing disc origin) in our analysis. Two other non-modENCODE cell lines—S2-DGRC and ovarian somatic sheath (OSS)—that are ordered frequently from the DGRC were also included.

Here, we present data supporting the utility of a genomic TE distribution (gTED) protocol to authenticate *D. melanogaster* cell lines. The developed gTED protocol was able to generate distinct TE genomic distribution signatures for all the cell lines tested. Moreover, using the gTED protocol, we were able to authenticate blinded samples from the *Drosophila* research community, thus validating the protocol. Moreover, the gTED signatures of up to 50 passages of S2R+ cells do not cluster in a passage-dependent manner, indicating that this protocol could be used to authenticate cell lines with up to 50 passages. Moving forward, we aim to expand the repertoire of cell lines assessed for their TE genomic distribution. We now have a protocol that can be adopted by the *Drosophila* research community to authenticate their cell lines and provide the necessary standards as per NIH guidelines.

Materials and methods

Drosophila cell lines and genomic DNA extraction

Our protocol development included six modENCODE lines derived from various *Drosophila* developmental stages: embryonic—S2R+ (DGRC #150, CVCL_Z831), S2-DRSC (DGRC #181, CVCL_Z992), Kc167 (DGRC #1, CVCL_Z834); L3 larval CNS origin—ML-DmBG3-c2 (DGRC #68, CVCL_Z728); larval circulatory system origin—*mbn2* (DGRC #147, CVCL_Z706); and wing disc origin—CME W1 Cl.8+ (DGRC #151, CVCL_Z790) (Table 1). Two other non-modENCODE cell lines—S2-DGRC (DGRC #6, CVCL_TZ72) and OSS (DGRC #190, CVCL_1B46)—were also included in the protocol development phase. The S2R+, S2-DRSC, S2-DGRC, *mbn2* cells were cultured in the Shields and Sang M3 medium (Sigma, Cat#: S8398) supplemented with 10% fetal bovine serum (FBS, Hyclone, GE Healthcare), bactopectone (Sigma), and yeast extract (Sigma) M3+BPYE + 10%FBS. ML-DmBG3-c2 cells were cultured in M3+BPYE + 10% FBS with 10 µg/ml insulin (Sigma-Aldrich), while CME W1 Cl.8+ cells required M3 + 2% FBS + 5 µg/ml insulin + 2.5% fly extract containing medium. OSS cells were cultured in M3 + 10% FBS + 10% fly extract with 60 mg L-glutathione (Sigma-Aldrich, Cat#: G6013) and 10 µg/ml insulin (Sigma-Aldrich, Cat#: I9278). Kc167 cells were cultured in CCM3 medium (Hyclone, Cat#: SH30061.03). To extract total genomic DNA (gDNA), cells were cultured to confluency, harvested by pipetting, centrifuged, and washed once with phosphate-buffered saline (PBS). gDNA was extracted from the PBS washed pellet using the Zymo Quick-DNA™ MiniprepPlusKit (Cat#: D4068/4069), using one column for every 10 million cells. gDNA was generated for triplicate samples of all cell lines in order to investigate the reproducibility of our

Table 1 Summary of transposable element (TE) insertions detected by gTED

Cell line	Tissue source	DGRC stock number	Cellosaurus ID	Number of TE insertions mean (\pm SD)
S2R+	Embryo	150	CVCL_Z831	1009 (\pm 30.4)
S2 DGRC	Embryo	6	CVCL_TZ72	704 (\pm 3.2)
mbn2	Larval circulatory system	147	CVCL_Z706	633 (\pm 6.4)
S2 DRSC	Embryo	181	CVCL_Z992	530 (\pm 14.8)
Kc167	Embryo	1	CVCL_Z834	516 (\pm 18.3)
OSS	Adult ovary	190	CVCL_1B46	404 (\pm 8.5)
CME-W1-Cl.8+	Larval wing disc	151	CVCL_Z790	309 (\pm 11.1)
ML-DmBG3-c2	Larval CNS	68	CVCL_Z728	227 (\pm 4.7)

The total number of TE insertions that were detected in each of the listed cell lines is presented as a mean ($n = 3$) of the samples analyzed. CNS, central nervous system; SD, standard deviation.

Table 2 List of blinded samples processed

Sample label	Source	Identification with gTED pipeline	Confirmation
DRSC_Blinded_1-3	DRSC	Kc167	Kc167
DRSC_Blinded_4-6	DRSC	No ID	A. g
DRSC_Blinded_7-9	DRSC	No ID	A. a
DRSC_Blinded_10-12	DRSC	Kc167	Kc167
DRSC_Blinded_13-15	DRSC	S2R+	S2R+
DRSC_Blinded_16-18	DRSC	S2	S2
SGLab_Blinded_1-3	Gorski Lab	mbn2	mbn2
SGLab_Blinded_4-6	Gorski Lab	S2	S2
DGRC_Blinded_A	Internal	No ID	1182-4H
DGRC_Blinded_B	Internal	No ID	Ras[V12]; wts[RNAi]
DGRC_Blinded_C	Internal	No ID	delta l(3)mbt-OSC

Blinded samples were donated by external (*Drosophila* RNAi Screening Center and Dr S. Gorski) or generated internally. The identifications were made upon processing the sample through the genomic TE distribution pipeline followed by computational analysis. No ID: The genomic TE signatures of the cell lines did not match with any of the lines analyzed to provide a positive identification. A. a: cell line derived from *Aedes aegypti*; A. g: cell line derived from *A. gambiae*.

protocol as well as to detect and mitigate potential mislabeling of individual samples during the project.

Blinded samples

External blinded samples from eight cell lines were obtained as triplicates of frozen gDNA samples extracted from insect cell lines from Dr Sharon Gorski, British Columbia Cancer Research Centre, Vancouver, Canada and the *Drosophila* RNAi Screening Center, Harvard University (Table 2). The identities of the external samples sent to DGRC were blinded by the sample donors. For internal blinded samples, gDNA was extracted from three cell lines in triplicate (Table 2). The identities of the internal samples were blinded from the team members involved in library preparation and downstream analyses. gDNA for both the external and internal blinded samples was extracted as per the protocol described above. The team members involved in library preparation and downstream analyses were blind to the identity and replicates of each sample.

Passage experiment

S2R+ cells were plated at 1×10^6 cells per ml at every passage. A single passage experiment was performed wherein cells were passaged every 2–3 days and replicates of the passages were frozen at the 1st, 10th, 20th, 30th, 40th, and 50th passages with the cell concentrations between 2.5 and 8.6×10^6 cells per ml. Triplicate gDNA samples from each passage was extracted as described above.

Primer design

Six TE families shown by Han et al. (2021) to be sufficient to identify *Drosophila* cell lines based on whole genome sequencing

(WGS) data were used as initial candidates for primer design. These six TE families are all LTR retrotransposons, which insert as full-length elements containing an identical LTR that provides a reliably known junction for PCR at each terminus of the TE (Smukowski Heil et al. 2021). Primer design was based upon the protocol outlined in Figure 1, involving a two-step PCR (Reaction A/B and Reaction A/B Nest PCR). Each step required one primer to be within the TE at either end (one for Reaction A at the 5' of the TE and one for Reaction B at the 3' of the TE). Additionally, primers for Reaction A/B and Reaction A/B Nest PCR needed to have low similarity. Based on these requirements, the general workflow for designing PCR primers for six diagnostic TE families for the eight focal cell lines was as follows:

Generate consensus sequences for LTRs of candidate TE families

- WGS data from Zhang et al. (2010), Lee et al. (2014), and Han et al. (2021) for all focal cell lines were mapped against TE canonical sequences and merged into a single BAM file.
- Variants were called on the merged BAM file and a VCF file was generated using bcftools call (v1.9).
- Full length consensus sequences for all six TE families from VCF file was generated using bcftools consensus (v1.9) with variable sites encoded as ambiguities.
- Both the 5' and 3' LTRs from the full-length TE consensus sequence for each family were extracted.

Detect the first round of primer candidates

Primers for nested PCR were detected with primer3 (v2.5.0) (<https://github.com/primer3-org/primer3>; last accessed: 11/28/2021) using the following parameters: PRIMER_LIBERAL_BASE=1; PRIMER_

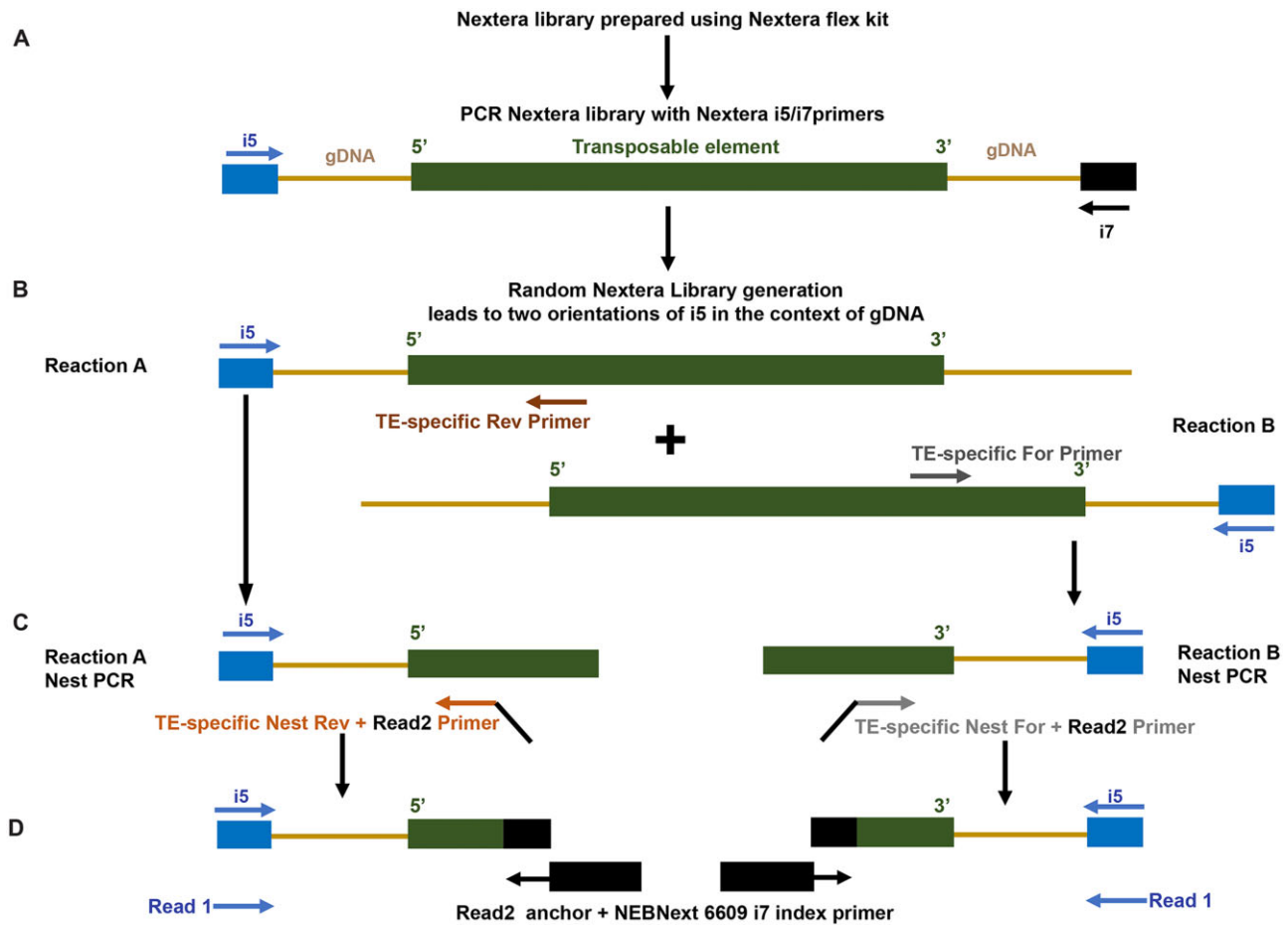


Figure 1 Protocol used for generating libraries to establish genomic transposable element distribution signatures. (A) Fragmented genomic DNA (gDNA; light brown lines) from the Nextera libraries containing TEs (green bar) and flanking gDNA were amplified with the randomly oriented i5 (blue arrow) and i7 (black arrow) primers. (B) Reactions A and B involved amplification with the i5 primer oriented in either direction with respect to the TE, in combination either with TE-specific Reverse (dark brown arrow) and Forward (dark gray arrow) primers, respectively. (C) The Nest PCR reactions amplified from within the products of the respective Reactions A and B using the i5 primer and either the TE-specific Nest Reverse (light brown arrow) or TE-specific Nest Forward (light gray arrow) primers. Read 2 anchors were added onto both the Nest PCR primers. (D) The final amplification step was performed with the i5 primer and the Read 2 anchor with the i7 index primer (black box). The reads from the genome sequences flanking the TE are designated as Read 1; the reads internal to the TE are designated Read 2.

MAX_NS_ACCEPTED=1; PRIMER_NUM_RETURN=10; PRIMER_GC_CLAMP=1; PRIMER_DNA_CONC=25; PRIMER_SALT_MONOVALENT=50; PRIMER_MIN_TM=60; PRIMER_OPT_TM=62; PRIMER_MAX_TM=65; PRIMER_SALT_DIVALENT=2; PRIMER_DNTP_CONC=0; PRIMER_TM_FORMULA=1

PRIMER_OPT_SIZE=22; PRIMER_MIN_SIZE=18; PRIMER_MAX_SIZE=25; PRIMER_MIN_GC=40; PRIMER_MAX_GC=60; PRIMER_PRODUCT_SIZE_RANGE=75-100 150-250 100-300 301-400 401-500 501-600 601-700 701-850 851-1000.

Detect the second round of non-overlapping primer candidates

The same parameters as in the previous round of primer design were used, with the additional specification that the primers designed in the first round were added to a “mispriming library” to exclude these regions for primer prediction in the second round of primer candidates.

Finalize primers from both rounds of primer candidates

The final primers for Reaction A/B PCR and Reaction A/B Nest PCR were selected from the candidate list from both rounds of primer design. Specifically, one primer was selected for Reaction

A/B PCR from either round of primer design, then another primer was selected for Reaction A/B Nest PCR from the other round of primer design.

Final adjustments to the primer locations were made based on testing the respective primer pairs. The full list of primers used in the study is listed in [Supplementary Table S1](#).

Nextera library preparation and nested PCR protocol

Nextera libraries were constructed for all the gDNA samples by using Nextera DNA Flex Library Prep Kit (Illumina, Cat#: 20018705) (Figure 1A). Then, the Nextera libraries were diluted into 1 nM, and 5 μ l of each was used as the template for the TE library construction. To amplify the fragments with the TE-specific genomic context, two separate multiplex PCRs were performed (Reactions A and B, Figure 1B) using TE-specific primers for all six families simultaneously in combination with the Illumina i5 primer. For Reactions A and B, two sets of primers (Forward and Reverse) were designed within the two LTRs of each of the TEs as detailed above. Since the generation of the Nextera library is not direction specific, DNA fragments can orient in either direction with respect to the i5 adaptor thus allowing for

detection at either ends of the TE by amplification with the Illumina i5 primer with a TE-specific primer. Therefore, this PCR step amplified the DNA fragments containing the 5' (Reaction A, Reverse primer) or 3' (Reaction B, Forward primer) flanking regions of the TEs. A second nested PCR was performed to enrich for the TE-gDNA junctions, utilizing nested primers from within the Reactions A and B with the i5 adaptor (Figure 1C). Both Nest PCR primers contained a specific overhang region (5'-GTTTCAGACGTGTGCTCTTCCGATCT-3') to facilitate addition of the index in the next PCR step. The final step was the Index PCR, which was performed to add the i7 adaptor and index by using the kit NEBNext® Multiplex Oligos for Illumina (cat: 6609S). Briefly, equal volumes of the products of Reactions A and B Nest PCRs containing either the TE 5' and 3' flanking regions were combined and used as the template. The Index PCR was performed by using the Illumina i5 primer and the NEBNext® Multiplex Oligos to add i7 adaptor and index (Figure 1D). Finally, the TE libraries were constructed with both i5 adaptors (added by Nextera library construction), i7 adaptors, and indexes (added by the Index adding PCR). A detailed nested PCR protocol is described in Supplementary File 1.

Sequencing

Paired end sequencing was performed on an Illumina NextSeq 500 with a 150-cycle midi-cycle kits. The first read in a pair (Read 1, R1) corresponds to flanking gDNA; the second read in a pair (Read 2, R2) corresponds to TE sequence. Raw sequencing data was submitted to SRA (SRP323476).

Sample processing and TE identification

Reads were trimmed for adapters and low quality using Trimmomatic (v0.38; ILLUMINACLIP:adapters.fa:3:20:6 LEADING:3 TRAILING:3 SLIDINGWINDOW:4:20 MINLEN:40). By design, R2 reads occur inside the TE and can be used to demultiplex individual fragments by TE of origin from a multiplex PCR. To do this, R2 reads were aligned to a database of the consensus sequences used for primer design of the relevant TEs using Bowtie2 (v2.3.5.1); the corresponding R1 reads from the same fragment were then demultiplexed into TE-specific bins based on the best alignment of R2. R1 reads were then mapped with Bowtie2 (-local -k 2) to the complement and reverse-complement *D. melanogaster* genome (version 6.30) in which the TEs were N-masked (Figure 2; red plus green reads). Masking was performed by searching consensus TEs sequences against the *D. melanogaster* genome (version 6.30) using NCBI blastn (version 2.2.26) with the following parameters: -a 10 -e 1e-100 -F "m L" -U T -K 20000 -b 20000 -m 8. R1 reads that did not map with a uniquely best match to the genome were subsequently excluded. Simultaneously, the R1 reads were mapped to the TE consensus sequences. The initial goal was to identify any valid junction where we could explicitly identify the transition from a unique genomic context into a TE, aka a TE junction (Figure 2; green reads). For a R1 read to identify a junction, the local alignment to the genome and the TE must be congruent such that the entire read was accounted for (± 2 bases). Valid junctions were defined such that multiple independent reads with independent start sites in the genome all identify the same breakpoint. To improve the sensitivity, all the data from all the different samples was combined for junction identification. A valid junction had to have at least 12 reads with 4 distinct start positions. Once the junctions were identified, 300 bp of genomic sequence outside and juxtaposed to the TE junction were isolated, which would include either 5' or 3' or both ends of the inserted TE (Figure 2).

Clustering and visualization

Read datasets were analyzed in their entirety or by random sub-sampling using vsearch (v2.14.2) (Rognes et al. 2016) down to 10 million reads, in order to control for sequencing depth and explore how many reads were necessary per cell line to produce reliable results. Read counts from sub-sampled datasets mapped to dm6 in the 300 bp intervals adjacent to TE junctions defined above were used to generate a binary matrix indicating the presence/absence of the TEs in any given sample. This binary matrix was constructed with custom code based on the observation that there are either many reads or very few reads per sample for any given TE insertion site. After normalizing the number of TE-associated reads per sample, a z-score was calculated for every TE across the samples. Positive z-scores were assigned as present and negative z-scores as absent. Because z-score normalization uses the mean of a sample, if all or most of the samples are positive, by definition, half of the samples would end up with a negative z-score. To avoid this mis-identification of positive samples, we add a dummy zero value to the set of samples for every real sample included before z-score calculation. These data were then visualized in R using the gplots function heatmap.2. The identities of blinded samples were estimated based on the clustering of these samples within the dendrogram derived from known samples.

Code

Code and notes on running the TE detection and clustering pipeline are available at: <https://github.com/mondegreen/DrosCellID>. git (last accessed: 11/28/2021).

Results

Drosophila cells have distinct TE signatures

Previous analysis of available WGS data revealed that gTED can reliably cluster cell lines based on their genotype and laboratory of origin (Han et al. 2021). Moreover, WGS analysis using a limited set of six TE families (297, *copia*, *mdg3*, *mdg1*, *roo*, and 1731) was sufficient to replicate the clustering observed when data from all TE families was used (Han et al. 2021). Nevertheless, an alternative approach that selectively enriches the six TE families would be more efficient and cost-effective. Therefore, based on these analyses, here we set out to determine if targeted identification of the genomic distribution of a small number of diagnostic TE families could be used to (1) build an authentication platform for *Drosophila* cell lines based on unique gTED signatures for each cell line, (2) test the validity of this protocol by assessing the identities of blinded samples, both internal and those provided by the *Drosophila* community, and (3) assess if cell lines subjected to extensive passaging retain the unique cell-specific gTED signatures.

To achieve these goals, we developed a novel TE-based next-generation sequencing (NGS) enrichment protocol described in the Materials and methods (Figure 1). Briefly, this protocol uses a multiplexed nested PCR approach to selectively amplify the library elements containing the 5' and 3' ends of the target TE families (Reaction A and B, Figure 1). The products from the final PCR amplification step were subjected to NGS and downstream analyses to determine the type of TE and identify the unique gDNA flanking the TE sequence.

The NGS data obtained was first used to identify TE junctions using the bioinformatic strategy outlined in Figure 2. Since the number of reads observed upon amplification with *mdg3*-specific primers was very low, *mdg3* was excluded from further analyses.

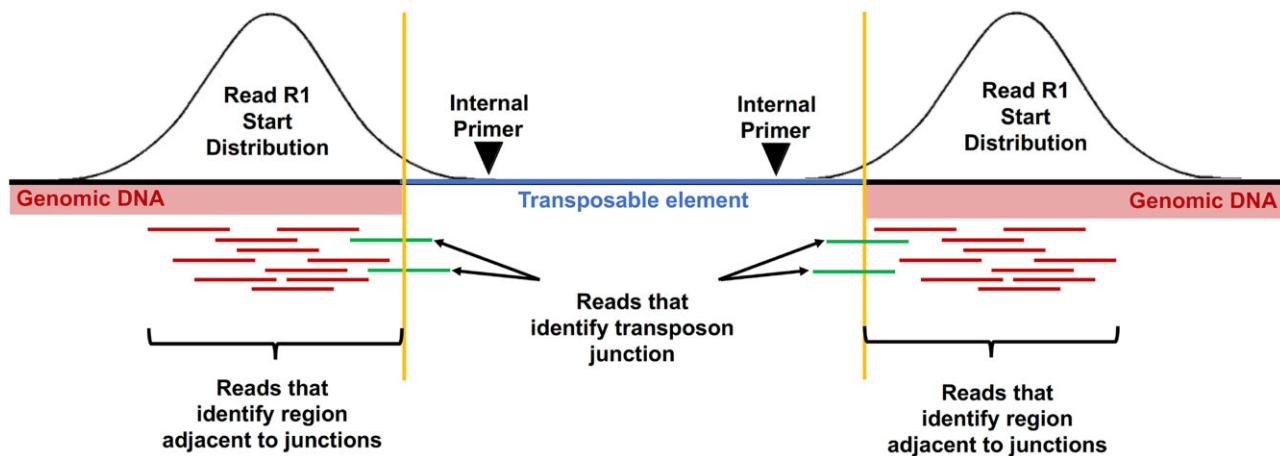


Figure 2 Read mapping strategy used to generate genomic transposable element distribution signatures. Read 1 (R1) reads from demultiplexed fragments were used to identify the transposon junctions (green) from the set of all R1 reads. The schematic represents R1 reads at junctions on either end (5' or 3') of a TE. The number of reads that specifically identify a junction is relatively small compared to the total number of reads near the junction. Variation in sequencing depth and subtle differences in the insert sizes produced by the Nextera library could cause junctions to be missed if only explicit junction calls are used. To avoid these issues, after the junctions have been identified, a 300-bp region of genomic sequence flanking the transposon is used to quantify the number of R1 reads (red) associated with that junction.

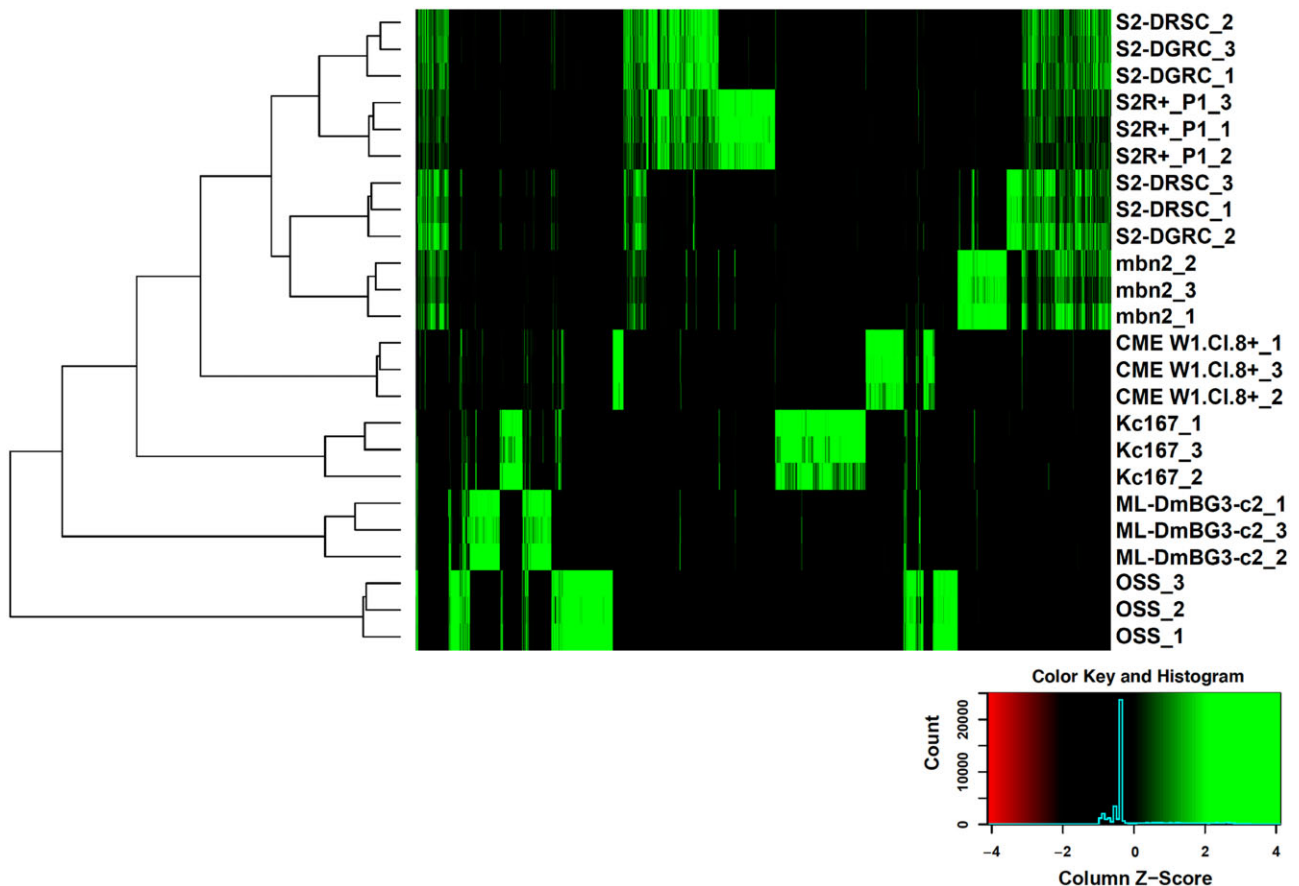


Figure 3 Clustering of cell lines based on genomic transposable element distribution. The cell line clustering was derived upon processing NGS data as described in the Materials and methods. The triplicates for each cell lines are indicated with 1–3 following the cell line name.

Normalized counts of reads mapping near TE junctions for the remaining five families were then used to hierarchically cluster all the cell lines. Reads mapping close to the identified TE junctions, whether at 5' or 3' end or both, were included in further analyses (Figure 2). The resulting dendrogram showed that the triplicate samples from most cell lines clustering together

(Figure 3). Upon processing the NGS data using an alternative approach (Supplementary File 2), a comparable clustering of all the samples was observed (Supplementary Figure S1). In both approaches, one replicate each from S2 DGRC (S2-DGRC_2) and S2 DRSC (S2-DRSC_2) did not cluster with the other replicates from these cell lines (Figure 3, Supplementary Figure S1). The

similar clustering from both bioinformatic approaches suggests the non-conforming clustering of these two replicates is not an artifact of genomic or computational methods, and was most likely caused by reciprocal sample mislabeling during gDNA extraction. Regardless of the cause of these two discrepancies, the majority of samples (2/3) for both S2 DGRC and S2 DRSC are respectively consistent with one another, providing confidence in the identity of these cell line clusters.

Distinct gTED signatures, a composite of the five TE families assessed, were observed for every cell line investigated (Figure 3 and Supplementary Figure S2). The tree visualization heatmap demonstrates that there are very few shared TE insertions between all cell lines (Figure 3). In general, the total number of TEs detected by this technique was higher in embryonic cell lines as opposed to cell lines derived from larval or adult tissues (Table 1, Supplementary Figure S2). The total number of TEs mapped was similar for the replicates of each of the cell lines as seen in the UpSET plot (Lex et al. 2014) for these samples (Supplementary Figure S2). For many of the cell lines, the majority of TE insertions detected were unique relative to those shared with other cell lines. For example, OSS replicates have 262 unique TEs that are not found in any other cell line investigated, with ≤ 9 TEs in common with any other individual cell lines (Supplementary Figure S2). The only lines that do not conform to having majority unique TE insertions are S2 DGRC and S2 DRSC as they share a considerable proportion of the TEs with S2R+ (Supplementary Figure S2). Nevertheless, unique patterns of gTED were sufficient to distinguish between the various S2 sublines (Figures 3, Supplementary Figures S1 and S2). Two of the three larval tissue-derived cell lines (ML-DmBG3-c2, mbn2, and CME W1 Cl.8+) have fewer genomic TE insertions as compared to embryonic S2 and Kc167 lines. However, mbn2, a cell line reportedly derived from the larval circulatory system (Gateff 1977; Gateff et al. 1980), has a gTED signature very close to those of the S2 lines, which are all of hematopoietic origin (Schneider 1972). The unexpected similarity between S2 lines and mbn2 was also described recently by Han et al. (2021) based on WGS-based TE distribution analysis. These analyses demonstrated that the protocol developed to determine genomic distribution of a set of five TE families in *Drosophila* cell lines can be utilized to create unique cell line-specific signatures.

TE signatures of *Drosophila* cell lines can be employed for authentication

To assess the value of the developed gTED pipeline and validate it, we next queried if the cell line-specific gTED signatures could be employed to determine the identities of blinded samples (Table 2). The blinded samples were either donations from the *Drosophila* community (external samples) or generated internally at DGRC. All blinded samples, as well as triplicates of an internal control for S2R+ (DGRC_Blinded_control_1-3), were processed as outlined in the *Materials and methods* section.

Of the eight external cell lines processed from two different donating labs, six robust gTED signatures were obtained (Supplementary Figure S3A). However, very few TE insertions detected in six samples, possibly from two cell lines (Supplementary Figure S3A). gTED profiles for three samples (DRSC_Blinded_13-15) were very similar to the internal control from S2R+ processed in this run (DGRC_Blinded_control_1-3, Supplementary Figure S3A). For 15 of the 18 samples with robust gTED profiles, clusters of triplicates were observed, indicating that each cluster possibly represents replicates samples of five cell lines (Figures 4 and Supplementary Figure S3A). One sample did not cluster distinctly with any of the other samples

(SGLab_Blinded_4, Figures 4 and Supplementary Figure S3A); however, this sample had a gTED profile that is visually most similar to samples SGLab_Blinded_5-6 (Supplementary Figure S3A). The six samples that had very few TE insertions (triplicates for each labeled DRSC_Blinded_4-6 and DRSC_Blinded_7-9) each passed the gDNA and library preparation quality control steps, and the consistent lack of TE insertions among replicates suggested that this was a reproducible signal. Upon clustering the external blinded samples with the previously characterized set of TE signatures, it was possible to predict the identities of these samples (Figure 4, Table 2) as DRSC_Blinded_1-3 and DRSC_Blinded_10-12 (Kc167), DRSC_Blinded_4-6 and DRSC_Blinded_7-9 (No identification), DRSC_Blinded_13-15 (S2R+), DRSC_Blinded_16-18 (S2), SGLab_Blinded_1-3 (mbn2), and SGLab_Blinded_5-6 (S2). Moreover, the clustering generated with gTED has the resolution to identify the various S2 sublines. For instance, it is evident that DRSC_Blinded_13-15 are closest to S2R+, DRSC_Blinded_16-18 to S2-DGRC, and SGLab_Blinded_5-6 to S2-DRSC (Figure 4). The investigators who donated the external samples confirmed that the identities determined by the gTED protocol were accurate for all the samples as predicted (Table 2). The two cell lines with very few TE insertions for which a cell line identity prediction could not be generated were mosquito cell lines (Figure 4, Table 2). These experiments demonstrated that the gTED protocol could reliably identify blinded *Drosophila* samples submitted to DGRC by the community.

All three internal blinded cell lines had unique gTED signatures that clustered distinctly relative to all previously characterized gTED signatures (Figures 4 and Supplementary Figure S3B). Nevertheless, the triplicates from each of the internal blinded cell lines reliably clustered together (Figure 4). Upon unblinding (Table 2), the internal blinded samples were found to be from three cell lines not included in the initial development phase of the project: 1182-4H (DGRC_Blinded_A, DGRC#177, CVCL_Z708), Ras[V12]; wts[RNAi] (DGRC_Blinded_B, DGRC#189, CVCL_IY71), and delta_l(3)mbt-OSC (DGRC_Blinded_C, DGRC#289). Thus, processing blinded samples through the gTED pipeline revealed that (1) reliable identification of samples with known gTED signatures can be achieved, (2) the protocol is capable of distinguishing *Drosophila* vs non-*Drosophila* cell lines, and (3) *D. melanogaster* cell lines previously uncharacterized by the gTED protocol can be identified as such, without providing a false identification.

TE signature of S2R+ is retained upon extensive passaging

Extensive passaging of cell lines can potentially alter cellular genomes (Wenger et al. 2004; Oh et al. 2013). Apart from gross genomic changes, extensive passaging introduced single nucleotide polymorphisms in mammalian cell lines (Pavlova et al. 2015). To determine the effect of extensive passaging on the gTED signatures generated in this study, we passaged S2R+ cell line 50 times and isolated gDNA in triplicate at every 10th passage for processing (Figure 5A). Upon generating a cluster using the gTED protocol, it is evident that the triplicates from the passages cluster randomly and not according to passage numbers (Figure 5B). Moreover, all replicates from every passage tested form a distinct cluster (Supplementary Figure S4) indicating that extensive passaging of S2R+ does not alter the S2R+ gTED signature for up to 50 passages.

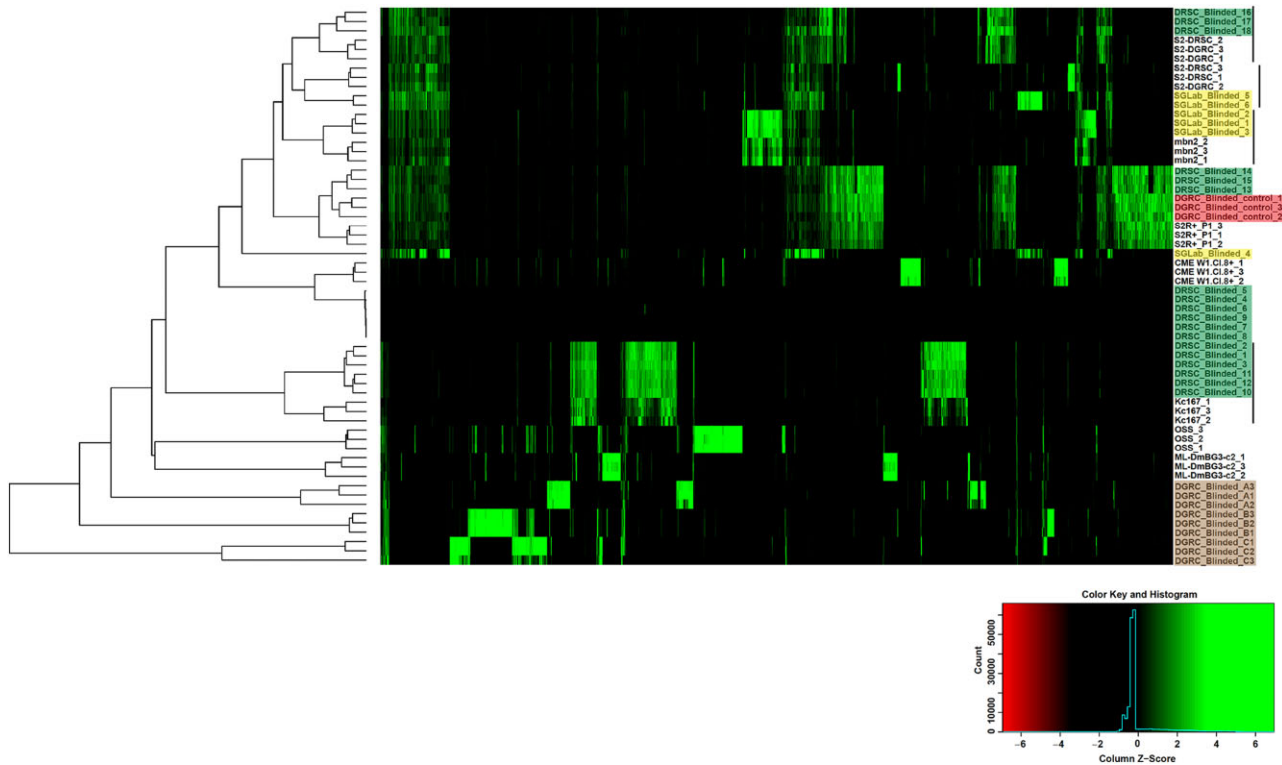


Figure 4 Cell line authentication of double-blind samples using genomic transposable element distribution signatures. Triplicate samples of external blinded cell lines from the lab of Dr S. Gorski (shaded yellow) and *Drosophila* RNAi Screening Center (shaded green) along with internal blinded samples (shaded brown) and internal control samples (shaded red) were processed with the gTED protocol (Figure 2B) and clustered as described in the Materials and methods along with the previously processed known samples. The cell lines that the blinded samples cluster with are indicated with the black lines. Internal blinded samples cluster as a separate group. Samples DRSC_Blinded_4-9 with very few or no TEs detected were from mosquito cell lines (Table 2).

Discussion

The aim of this study was to develop and test a cell authentication protocol that could reliably identify the most commonly used *Drosophila* cell lines to help researchers validate their reagents as per the NIH mandate. Our novel protocol allowed us to define unique gTED signatures that could identify each of the *Drosophila* cell lines that were tested here. In addition, the resolution obtained from the gTED signatures allows for distinguishing between S2 sublines. Data presented here demonstrate that the gTED signatures of the replicates of most cell lines cluster together, outlining the reproducibility of the gTED protocol while also underscoring the value of having replicate samples for reliable cell line identification. Crucially, accurate identification of blinded samples donated by the research community validated the gTED protocol in a real-world setting.

To reliably identify a *D. melanogaster* cell line using the gTED protocol, an established gTED signature is a prerequisite. Toward this end, we have now established gTED signatures for the widely distributed lines, S2R+, S2 DGRC, S2 DRSC, Kc167, and ML-DmBG3-c2 lines (Luhur et al. 2019). In addition, gTED signatures are also available for OSS, mbn2, CME W1 Cl.8+, 1182-4H, Ras[V12]; wts[RNAi]; and delta 1(3)mbt-OSC lines. Importantly, the lack of an established gTED signature does not lead to misidentification, as was observed with the internal blinded samples. In the event that a cell line without an established gTED signature needs to be authenticated, a stock from the DGRC repository with the same identity will be assayed concurrently to serve as a control. In due course, DGRC will also expand the gTED protocol

to include as many cell lines from our repository as possible. These efforts will ensure the creation of a comprehensive database of gTED signatures for *Drosophila* cell lines.

Mosquito cell lines included as blinded samples helped clarify that the gTED protocol can discriminate non-*Drosophila* cell lines. In *Aedes aegypti* and *Anopheles gambiae*, 10% and 6% of the total genome, respectively, is comprised of LTR retrotransposons (Nene et al. 2007; Melo and Wallau 2020). Presence of active LTR transposons, specifically Ty1/copia, has also been described in Aag2 (*A. aegypti*) cells (Maringer et al. 2017). Since we confirmed that the DNA and library preparation for these samples were comparable, it is most likely therefore that the TE-specific primers used in this study cannot amplify mosquito TE families. Our results demonstrate that in pure samples, mosquito cells can be distinguished from *D. melanogaster* cell lines using the gTED protocol. However, detecting low levels of inter- or intra-species contamination might be a more challenging pursuit. A *D. melanogaster* cell line contaminated with low levels of a mosquito cell line is unlikely to be detected with gTED, necessitating using other methods for such specific instances. A future avenue is to explore the sensitivity of the gTED protocol to intra- or inter-species contamination. In addition, it will be imperative to determine if we can determine low levels of contamination of *Drosophila* cell lines containing unique gTED signatures.

Our analysis also demonstrated that the genomic distribution of TEs is largely unchanged over 50 passages in S2R+ cells. The narrow window into the passaging-associated genomic structure provided by the gTED protocol is most likely not representative of more complex genomic and/or transcriptomic changes that the

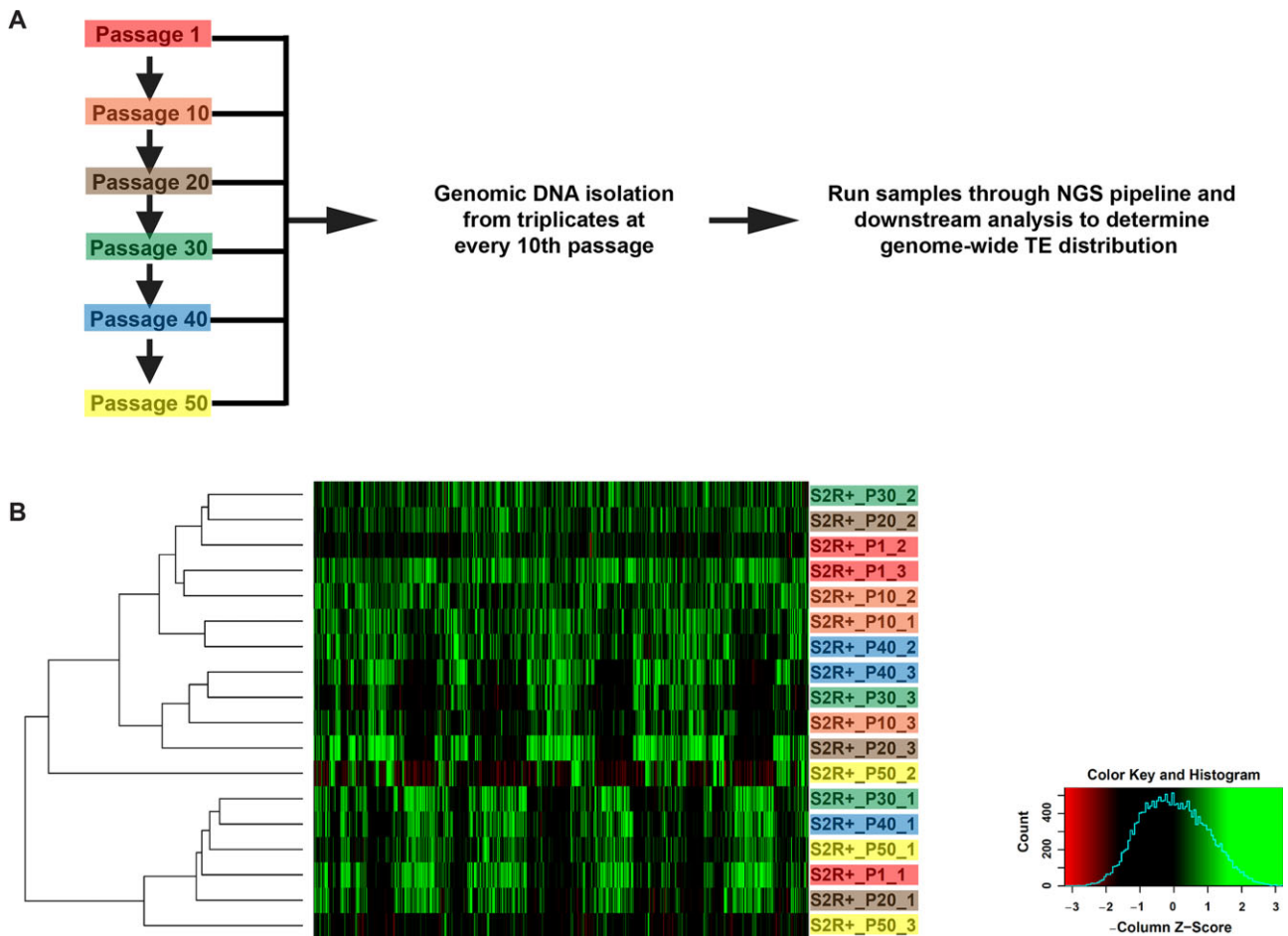


Figure 5 Genomic transposable element distribution signatures for S2R+ cells do not cluster by passage number. (A) Schematic outlining the protocol to acquire samples between 1 and 50 S2R+ passages for assessment by the gTED protocol. (B) Clustering of all the passage samples generated based on TE predictions. The triplicates samples of every passage are shaded in one color each.

extensively passaged cells might have undergone. Nevertheless, S2R+ cells passaged continuously for up to 50 times can still be identified with the gTED protocol. Among the S2 lines assessed in this study, it has been proposed that the S2R+ line is possibly the closest to the original Schneider line (Schneider 1972; Yanagawa et al. 1998). The other two S2 sublines, S2-DGRC and S2-DRSC, are isolates with less clear history from the original Schneider isolates before being added to the DGRC repository (Ayer and Benyajati 1992; Cherry et al. 2005). All three of the S2 sublines assessed have unique gTED signatures that discriminate them and can be used to identify blinded cell lines precisely to the S2 subline. In general, S2 sublines have a more complex TE-landscape, higher aneuploidy, and copy number variation than other *D. melanogaster* cell lines (Han et al. 2021). The possibility that the gTED signature can be used as a proxy for broader genomic changes remains to be investigated.

The gTED protocol relies on TE-specific amplification from gDNA and therefore provides a cost-effective strategy as compared to performing WGS for the same purpose. In addition, post-sequencing downstream analyses can be performed more quickly because of the smaller amount of sequencing data produced by the gTED protocol. The reduced cost and computing time requirements of the gTED protocol allowed multiple triplicate sample processing, thus aiding the resolution of sample mislabeling that was detected with

one of the replicates of S2 DGRC and S2 DRSC (Figure 3, Supplementary Figure S1).

In summary, utilizing the genomic distribution of five TE families, we have developed the gTED pipeline to facilitate the authentication of *Drosophila* cell lines. We demonstrate that the developed gTED protocol can assign distinct signatures to the various *Drosophila* cell lines tested. Blinded and extensively passaged samples can now be authenticated employing the gTED protocol. Researchers working with *Drosophila* cell lines can independently authenticate cell lines being used in their laboratories using the protocol and code described in this study. Alternatively, DGRC will implement a cost-based service for the research community to access and authenticate their cell lines for both publications and research funding. Ultimately, our goal is to include more cell lines from the DGRC repository into the gTED pipeline and generate gTED signatures for all cell lines deposited with the DGRC.

Data availability

All data necessary for confirming the conclusions in this paper are included in this article and in Supplementary figures and tables. All the NGS data has been deposited at Sequence Read Archive available with the accession number: SRP323476.

Supplementary material is available at G3 online.

Acknowledgments

We thank Dr Kris Klueg for critical input in shaping the manuscript. We thank Grace Kim (DRSC), Dr Stephanie Mohr (DRSC), Nancy Erro Go (British Columbia Cancer Research Centre), and Dr Sharon Gorski (British Columbia Cancer Research Centre) for providing the blinded genomic DNA samples. We thank Chunlin Yang, Jie Huang, and Dr Sumitha Nallu at the Center for Genomics and Bioinformatics (Indiana University, Bloomington) for their help with NGS sample processing.

Funding

This work was supported by National Institutes of Health grants (5P40OD010949 and 3P40OD010949-16S2) to the *Drosophila* Genomics Resource Center, National Science Foundation under Grant No. CNS-0521433 to Center for Genomics and Bioinformatics (Indiana University, Bloomington) and the University of Georgia Research Foundation to C.M.B.

Conflicts of interest

The authors declare that there is no conflict of interest.

Literature cited

- Aguilera-Gomez A, Zacharogianni M, van Oorschot MM, Genau H, Grond R, et al. 2017. Phospho-rasputin stabilization by Sec16 is required for stress granule formation upon amino acid starvation. *Cell Rep.* 20:2277.
- Albert EA, Bokel C. 2017. A cell based, high throughput assay for quantitative analysis of Hedgehog pathway activation using a Smoothed activation sensor. *Sci Rep.* 7:14341.
- Almeida JL, Cole KD, Plant AL. 2016. Standards for cell line authentication and beyond. *PLoS Biol.* 14:e1002476.
- ATCC 2011. Authentication of Human Cell Lines: Standardization of STR Profiling. Washington, DC: ANSI.
- Ayer S, Benyajati C. 1992. The binding site of a steroid hormone receptor-like protein within the *Drosophila* Adh adult enhancer is required for high levels of tissue-specific alcohol dehydrogenase expression. *Mol Cell Biol.* 12:661–673.
- Bairoch A. 2018. The Cellosaurus, a cell-line knowledge resource. *J Biomol Tech.* 29:25–38.
- Ben-David U, Siranosian B, Ha G, Tang H, Oren Y, et al. 2018. Genetic and transcriptional evolution alters cancer cell line drug response. *Nature.* 560:325–330.
- Bergman CM, Bensasson D. 2007. Recent LTR retrotransposon insertion contrasts with waves of non-LTR insertion since speciation in *Drosophila melanogaster*. *Proc Natl Acad Sci U S A.* 104:11340–11345.
- Capes-Davis A, Theodosopoulos G, Atkin I, Drexler HG, Kohara A, et al. 2010. Check your cultures! A list of cross-contaminated or misidentified cell lines. *Int J Cancer.* 127:1–8.
- Charlesworth B, Langley CH. 1989. The population genetics of *Drosophila* transposable elements. *Annu Rev Genet.* 23:251–287.
- Cherbas L, Willingham A, Zhang D, Yang L, Zou Y, et al. 2011. The transcriptional diversity of 25 *Drosophila* cell lines. *Genome Res.* 21:301–314.
- Cherry S, Doukas T, Armknecht S, Whelan S, Wang H, et al. 2005. Genome-wide RNAi screen reveals a specific sensitivity of IRES-containing RNA viruses to host translation inhibition. *Genes Dev.* 19:445–452.
- Cridland JM, Macdonald SJ, Long AD, Thornton KR. 2013. Abundance and distribution of transposable elements in two *Drosophila* QTL mapping resources. *Mol Biol Evol.* 30:2311–2327.
- Gateff E. 1977. Malignant neoplasms of the hematopoietic system in three mutants of *Drosophila melanogaster*. *Ann Parasitol Hum Comp.* 52:81–83.
- Gateff E, Gissmann L, Shrestha R, Plus N, Pfister H, et al. 1980. Characterization of two tumorous blood cell lines of *Drosophila melanogaster* and the viruses they contain. In: Kurstak E, Maramorosch K, and Dübendorfer A. (eds). *Invertebrate Systems in Vitro*. Amsterdam: Elsevier/ North-Holland Biomedical Press, p. 517–533.
- Han S, Basting PJ, Dias G, Luhur A, Zelhof AC, et al. 2021. Transposable element profiles reveal cell line identity and loss of heterozygosity in *Drosophila* cell culture. *Genetics.* 219: iyab113.
- Kharchenko PV, Alekseyenko AA, Schwartz YB, Minoda A, Riddle NC, et al. 2011. Comprehensive analysis of the chromatin landscape in *Drosophila melanogaster*. *Nature.* 471:480–485.
- Lee H, McManus CJ, Cho DY, Eaton M, Renda F, et al. 2014. DNA copy number evolution in *Drosophila* cell lines. *Genome Biol.* 15:R70.
- Lex A, Gehlenborg N, Strobel H, Vuilleumot R, Pfister H. 2014. UpSet: visualization of intersecting sets. *IEEE Trans Vis Comput Graph.* 20:1983–1992.
- Liu Y, Mi Y, Mueller T, Kreibich S, Williams EG, et al. 2019. Multi-omic measurements of heterogeneity in HeLa cells across laboratories. *Nat Biotechnol.* 37:314–322.
- Luhur A, Klueg KM, Zelhof AC. 2019. Generating and working with *Drosophila* cell cultures: current challenges and opportunities. *Wiley Interdiscip Rev Dev Biol.* 8:e339.
- Maringer K, Yousuf A, Heesom KJ, Fan J, Lee D, et al. 2017. Proteomics informed by transcriptomics for characterising active transposable elements and genome annotation in *Aedes aegypti*. *BMC Genomics.* 18:101.
- Melo ESD, Wallau GL. 2020. Mosquito genomes are frequently invaded by transposable elements through horizontal transfer. *PLoS Genet.* 16:e1008946.
- Mohr SE, Rudd K, Hu Y, Song WR, Gilly Q, et al. 2018. Zinc detoxification: a functional genomics and transcriptomics analysis in *Drosophila melanogaster* cultured cells. *G3 (Bethesda).* 8:631–641.
- Nene V, Wortman JR, Lawson D, Haas B, Kodira C, et al. 2007. Genome sequence of *Aedes aegypti*, a major arbovirus vector. *Science.* 316:1718–1723.
- NIH. 2015. Enhanced Reproducibility through Rigor and Transparency. Bethesda, MD: NIH.
- NIH Rigor and Reproducibility. 2014. Principles and Guidelines for Reporting Preclinical Research and Endorsement by major journals. <http://www.nih.gov/research-training/rigor-reproducibility/principles-guidelines-reporting-preclinical-research> (Accessed: 2021 November 28).
- Nonaka S, Ando Y, Kanetani T, Hoshi C, Nakai Y, et al. 2017. Signaling pathway for phagocyte priming upon encounter with apoptotic cells. *J Biol Chem.* 292:8059–8072.
- Oh JH, Kim YJ, Moon S, Nam HY, Jeon JP, Lee JH, et al. 2013. Genotype instability during long-term subculture of lymphoblastoid cell lines. *J Hum Genet.* 58:16–20.
- Ozkan E, Carrillo RA, Eastman CL, Weiszmann R, Waghray D, et al. 2013. An extracellular interactome of immunoglobulin and LRR proteins reveals receptor-ligand networks. *Cell.* 154:228–239.
- Pavlova GV, Vergun AA, Rybalkina EY, Butovskaya PR, Ryskov AP. 2015. Identification of structural DNA variations in human cell cultures after long-term passage. *Cell Cycle.* 14:200–205.

- Potter SS, Brorein WJ, Jr, Dunsmuir P, Rubin GM. 1979. Transposition of elements of the 412, copia and 297 dispersed repeated gene families in *Drosophila*. *Cell*. 17:415–427.
- Rahman R, Chirn GW, Kanodia A, Sytnikova YA, Brembs B, et al. 2015. Unique transposon landscapes are pervasive across *Drosophila melanogaster* genomes. *Nucleic Acids Res*. 43:10655–10672.
- Rognes T, Flouri T, Nichols B, Quince C, Mahe F. 2016. VSEARCH: a versatile open source tool for metagenomics. *PeerJ*. 4:e2584.
- Schneider I. 1972. Cell lines derived from late embryonic stages of *Drosophila melanogaster*. *J Embryol Exp Morphol*. 27:353–365.
- Schug MD, Mackay TF, Aquadro CF. 1997. Low mutation rates of microsatellite loci in *Drosophila melanogaster*. *Nat Genet*. 15:99–102.
- Smukowski Heil C, Patterson K, Hickey AS-M, Alcantara E, Dunham MJ. 2021. Transposable element mobilization in interspecific yeast hybrids. *Genome Biol Evol*. 13:evab033.
- Tsuyama T, Tsubouchi A, Usui T, Imamura H, Uemura T. 2017. Mitochondrial dysfunction induces dendritic loss via eIF2alpha phosphorylation. *J Cell Biol*. 216:815–834.
- Wenger SL, Senft JR, Sargent LM, Bamezai R, Bairwa N, et al. 2004. Comparison of established cell lines at different passages by karyotype and comparative genomic hybridization. *Biosci Rep*. 24:631–639.
- Yanagawa S, Lee JS, Ishimoto A. 1998. Identification and characterization of a novel line of *Drosophila* Schneider S2 cells that respond to wingless signaling. *J Biol Chem*. 273:32353–32359.
- Yang D, Li N, Zhang G. 2018. Spontaneous adipogenic differentiation potential of adiposederived stem cells decreased with increasing cell passages. *Mol Med Rep*. 17:6109–6115.
- Zhang Y, Malone JH, Powell SK, Periwal V, Spana E, et al. 2010. Expression in aneuploid *Drosophila* S2 cells. *PLoS Biol*. 8:e1000320.

Communicating editor: B. Oliver